Dimers of Fluorinated Methanes with Carbonyl Sulfide: The Rotational Spectrum and Structure of Difluoromethane−OCS

Michal M. Serafin and Sean A. Peebles*

Department of Chemistry, Eastern Illinois University, 600 Lincoln Avenue, Charleston, Illinois 61920

Received: August 13, 2008; Revised Manuscript Received: October 21, 2008

The pure rotational spectra of four isotopologues of the difluoromethane−carbonyl sulfide dimer have been measured in the 5−15 GHz region with use of pulsed-nozzle Fourier-transform microwave spectroscopy. The complex was determined to possess an *ab* plane of symmetry with a center of mass separation of 3.41(2) Å and dipole moment components $\mu_a = 1.1386(18)$ D, $\mu_b = 0.4840(63)$ D, $\mu_{total} = 1.2372(41)$ D. Experimental planar moments indicate that the two fluorine atoms straddle the symmetry plane while one of the C−H bonds of the difluoromethane monomer is aligned to interact with the oxygen atom of the OCS molecule. The assignment of the rotational spectrum for this dimer completes the experimental studies of the series of dimers involving fluorinated methanes (HCF_3, H_2CF_2, and H_3CF) complexed with OCS and makes possible a comparison of properties within this series.

I. Introduction

Structural parameters have been reported recently for the trifluoromethane−carbonyl sulfide[1] (TFM−OCS), methyl fluoride−carbonyl sulfide[2] (FM−OCS), and trifluoromethane−carbon dioxide[3] (TFM−CO_2) weakly bound complexes as part of a systematic study aiming to characterize weak intermolecular interactions by examining the characteristics of the interaction of fluorinated methanes with simple linear molecules as the degree of fluorination is varied. To complete the series of OCS complexes, the rotational spectra of four isotopologues of the difluoromethane−carbonyl sulfide (H_2CF_2−OCS) dimer have now been recorded using Fourier-transform microwave (FTMW) spectroscopy and a structure has been determined.

Rotational spectra for several binary complexes[4–8] (and one ternary complex[9]) involving difluoromethane (H_2CF_2, DFM) have previously been measured, as well as rare gas dimers of DFM complexed with Ar,[10] Kr,[11] and Xe.[12] In some of these complexes, multiple interactions are observed between the DFM subunit and the other monomer. For instance, in the DFM dimer three C−H···F links are formed between the two DFM molecules,[5,6] while nine such interactions were observed in the DFM trimer.[9] These multiple links typically serve to increase the barrier to internal rotation of the DFM subunit by increasing the strength of binding between the monomers. Interestingly, the rotational spectrum of the DFM−oxirane system[4] displays a low-energy conformation where both hydrogen atoms of the DFM subunit hydrogen bond simultaneously to the oxygen atom of the oxirane subunit. The two lowest energy ab initio structures obtained for the DFM−OCS complex in the present study exhibit either one or two C−H···O contacts and so it was of interest to see whether an analogous doubly hydrogen bonded form of DFM−OCS could be isolated experimentally.

II. Experimental Section

The rotational spectra of the normal and three singly substituted isotopologues of the DFM−OCS weakly bound dimer were measured on a Balle-Flygare Fourier-transform microwave spectrometer.[13,14] The resonant cavity of this instrument is formed by mirrors of 41 cm diameter with a radius of curvature of 91 cm and a variable separation of 55−60 cm. Gas samples consisted of about 1% of each component stored in a 2 L glass bulb, diluted to a total pressure of 2−2.5 atm with "first-run" He/Ne carrier gas (17.5% He: 82.5% Ne, BOC gases); this sample was subsequently expanded into the cavity (perpendicular to the direction of microwave propagation) at a 10 Hz repetition rate via a General Valve Series 9 solenoid valve with a 0.8 mm orifice. The H_2CF_2−$O^{13}CS$ spectrum was measured by using an isotopically enriched sample ($O^{13}CS$, 99% atom ^{13}C, Icon Isotopes) while the spectra of the H_2CF_2−$OC^{34}S$ and $H_2{}^{13}CF_2$−OCS species were measured in natural abundance (4.2% and 1.1%, respectively). Dipole moment measurements were made by application of electric potentials of up to ±5 kV to a pair of steel mesh plates located 31 cm apart and straddling the supersonic jet expansion within the Fabry-Pérot cavity. Electric field calibration was carried out using the $J = 1 \rightarrow 0$ transition of carbonyl sulfide, assuming a dipole moment of 0.71519(3) D.[15]

III. Results

Ab Initio Optimizations. Gaussian 03[16] geometry optimizations were initially used to identify the lowest energy structures of DFM-OCS at the MP2/6-311++G(2d,2p) level prior to the spectroscopic searches; these structures are shown in Figure 1, and denoted hereafter as structures I and II. Structure I was determined to be the most stable arrangement while structure II was calculated to lie 73 cm^{-1} higher in energy than structure I (using energies uncorrected for basis set superposition error (BSSE) and zero point energy (ZPE)); the theoretical rotational constants and structural parameters for both ab initio structures are given in Table 1. Inspection of these two structures shows that these two species are not simply related by a straightforward 90° rotation about the C_2 axis of the fluorinated methane unit and they also have very different extensions of mass out of the symmetry plane (as highlighted by the planar moments (Table 1)), suggesting that it may be possible to isolate both species in the supersonic jet expansion.

* Corresponding author. E-mail: sapeebles@eiu.edu. Phone: (217) 581-2679. Fax: (217) 581-6613.

10.1021/jp8072393 CCC: $40.75
Published on Web 11/13/2008

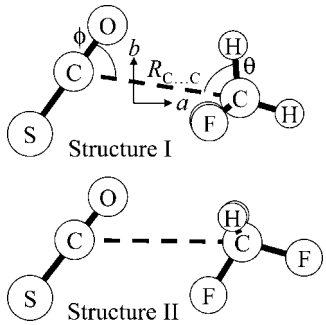

Figure 1. The two structures (I and II) obtained from the MP2/6-311++G(2d,2p) optimizations of H_2CF_2-OCS. Structure I is the lowest energy structure.

TABLE 1: Structural Parameters, Rotational Constants, Planar Moments, and Dipole Moment Components Obtained from the ab Initio (MP2/6-311++G(2d,2p)) Optimizations on Structures I and II (Structural Parameters Are Defined in Figure 1)

parameter	structure I	structure II
$R_{C\cdots C}$/Å	3.45	3.61
θ/deg	74.9	58.4[a]
ϕ/deg	63.8	53.4
A/MHz	4480	7597
B/MHz	1333	914
C/MHz	1266	820
P_{aa}/u Å^2 [b]	332.8	551.4
P_{bb}/u Å^2	66.44	64.95
P_{cc}/u Å^2	46.37	1.569
μ_a/D	1.18	1.28
μ_b/D	0.52	1.20
μ_c/D	0.00	0.00
μ_{total}/D	1.29	1.75
rel energy/cm^{-1}	0	73

[a] The angle θ in structure II is defined as the angle C···C−F (where the F atom is the in-plane fluorine atom closest to the OCS subunit) [b] The second moments are defined as follows: $P_{aa} = 0.5(I_b + I_c - I_a) = \sum_i m_i a_i^2$, etc.

Rotational Spectra. The search regions were rich in transitions due to the existence of several additional species that were significantly populated in our supersonic expansion; clusters containing only DFM (DFM dimer and trimer) were particularly intense.[5,6,9] Nevertheless, the most intense lines in the search region (having a signal-to-noise ratio in excess of 60 for measurements of 50 averaged gas pulses) belonged to the DFM−OCS complex, and were of sufficiently high intensity that several rotational transitions for the ^{34}S species were easily observed in natural abundance during our initial 50 shot fast scan.

The near-prolate nature of the DFM−OCS dimer ($\kappa = -0.960$) made the identification of the intense *a*-type spectrum relatively straightforward. The measured transitions (see the Supporting Information) were fit to a Watson *A*-reduction Hamiltonian in the I^r representation, using Pickett's SPFIT[17] program, and the derived spectroscopic constants are displayed in Table 2. The P_{cc} planar moments for all the isotopic species are also tabulated in Table 2; for each isotopologue the P_{cc} value obtained from the rotational constants confirms that it is the two fluorine atoms of the DFM that lie out of the *ab* plane of symmetry, as predicted by the lowest energy ab initio structure I (this will be discussed further in the Structure and Binding section below). Several rotational transitions still remain unassigned in the initial search region; it is possible that some of these may belong to structure II of DFM-OCS, or perhaps to the Ne−DFM complex, and these possibilities are being pursued.

Structure and Binding. The calculation of P_{cc} planar moments from the experimental moments of inertia describes the mass located out of the *ab* plane of symmetry ($P_{cc} = 0.5(I_a + I_b - I_c) = \sum_i m_i c_i^2$, where c_i is the coordinate of atom *i* on the *c*-axis). The values obtained from the rotational constants are approximately 45.45 u Å^2 for all four isotopologues (see Table 2). The proximity of this P_{cc} second moment for the dimer to the P_{aa} value of the DFM monomer (46.00436 u Å^2)[18] clearly indicates that the F atoms straddle the *ab* plane confirming structure I as the experimentally observed species (since structure II, with the H atoms located out of the plane, would naturally require a considerably smaller second moment (closer to the P_{cc} value of 1.65175 u Å^2 for DFM monomer)).[18]

Assuming therefore that the DFM−OCS complex possesses an *ab* plane of symmetry, and that the monomer structures are fixed to their literature values,[19] only three structural parameters need to be defined to describe the dimer geometry (as shown in Figure 1). These three structural parameters are two tilt angles for the relative alignment of the two monomers (θ, ϕ) and an intermolecular separation (chosen here to be the distance between the two carbon atoms ($R_{C\cdots C}$)). Several least-squares fits of these parameters to obtain the best reproduction of the experimental moments of inertia were carried out with use of the STRFITQ program of Schwendeman[20] and the results are shown in Table 3. Since only two moments of inertia for each isotopologue are truly independent in this system, pairs of moments of inertia were fitted as well as fitting all three moments of inertia for each species. The angle describing the orientation of the DFM subunit exhibits a slightly larger than desired uncertainty because no isotopic substitution data for the H atom positions were obtained due to the lack of commercially available sources for a deuterated sample of DFM (D_2CF_2 or $HDCF_2$). By variation of the particular set of the moments of inertia that are utilized in the inertial fit, it is possible to obtain best fit values for the three structural parameters, and these values are summarized in Table 3; note that the variation among the parameters obtained from the different sets of moments of inertia is small.

The principal axis coordinates for the substituted atoms were determined from a Kraitchman single isotopic substitution calculation[21] by using Kisiel's KRA program[22] and are compared to the resulting coordinates from our inertial fit and to the ab initio coordinates for structures I and II in Table 4, showing agreement to within 0.05 Å at worst for the ab initio values and even better agreement with the inertial fit structure coordinates. The derived Kraitchman coordinates can be used to determine the C═S bond distance of OCS in the dimer giving a C═S bond length of 1.568(3) Å, which is in excellent agreement with the literature value of 1.5651 Å.[19] A C···C═S bond angle of 114.7(2)° can also be calculated from the substitution coordinates, giving a value of the O−C···C angle of 65.3(2)°, again in excellent agreement with the inertial fit angle of 65.0(5)°. The substitution value of the C···C distance is also very reasonable, giving 3.548(2) Å from the Kraitchman coordinates, compared to the best estimate of 3.58(2) Å resulting from the inertial fits (despite the very small *b*-coordinate of the carbon atom in the DFM subunit that amplifies the uncertainties in the calculated substitution distance). Note that the determination of the *c*-coordinates of all three substituted atoms gave small, imaginary values—these were assumed to be zero in the above calculations.

TABLE 2: Spectroscopic Constants of the Normal and Isotopically Substituted Species of the H_2CF_2−OCS Complex[a]

	H_2CF_2−OCS	$H_2{}^{13}CF_2$−OCS	H_2CF_2−$O^{13}CS$	H_2CF_2−$OC^{34}S$
A/MHz	4505.6740(27)	4505.5025(35)	4489.7386(9)	4472.3799(18)
B/MHz	1277.0710(27)	1261.1336(12)	1271.9949(7)	1248.8408(9)
C/MHz	1212.0064(27)	1197.6236(9)	1206.2624(7)	1184.1930(7)
Δ_J/kHz	5.0345(86)	4.8726(94)	4.978(11)	4.841(13)
Δ_{JK}/kHz	13.386(48)	13.64(20)	13.15(6)	12.08(20)
Δ_K/kHz	21.72(52)	21.72[b]	21.72[b]	21.72[b]
δ_J/kHz	0.5906(43)	0.567(11)	0.598(15)	0.554(10)
δ_K/kHz	−59.3(14)	−59.3 [b]	−59.3[b]	−59.3[b]
$\Delta\nu_{rms}$/kHz[c]	1.7	3.6	1.7	3.0
N[d]	42	14	25	15
P_{cc}/u Å^2 [e]	45.4604(9)	45.4592(4)	45.4563(2)	45.4539(3)

[a] Uncertainties are the a priori errors reported by the SPFIT program. [b] Distortion constants Δ_{JK} and δ_K were fixed at the value obtained for the normal isotopic species. [c] $\Delta\nu_{rms} = [\sum(\nu_{obs} - \nu_{calc})^2/N]^{1/2}$. [d] Number of fitted transitions. [e] Second moment, $P_{cc} = 0.5(I_a + I_b - I_c) = \sum_i m_i c_i^2$.

TABLE 3: Fitted Structural Parameters for the H_2CF_2−OCS Dimer with Different Sets of Moments of Inertia[c]

	$R_{C\cdots C}$/Å	$R_{O\cdots H}$/Å [a]	θ/deg	ϕ/ deg	std dev/u Å^2
I_a, I_b, I_c	3.583(82)	2.89(20)	79(10)	65.0(22)	0.400
I_a, I_b	3.586(16)	2.910(40)	80.1(19)	64.95(43)	0.057
I_a, I_c	3.583(16)	2.882(40)	79.1(19)	64.69(43)	0.052
I_b, I_c	3.579(9)	2.863(21)	77.8(10)	65.22(23)	0.043
best fit[b]	3.58(2)	2.88(3)	79(2)	65.0(5)	

[a] The $R_{O\cdots H}$ distance is derived from the other three fitted structural parameters ($R_{C\cdots C}$, θ, and ϕ). [b] The "best fit" value is an attempt to incorporate all the values in the above table into a best guess value that provides a more realistic uncertainty for each parameter. [c] See Figure 1 for the definition of the structural parameters.

TABLE 4: Principal Axis Coordinates[a] Derived from the Kraitchman Single Substitution Calculations, Inertial Fit, and ab Initio Optimizations (all values are in angstroms)[c]

	principal axis coordinates[b]/Å		
	a	*b*	*c*
$H_2{}^{13}CF_2$	2.2428(7)	0.075(21)	0.035*i*(44)
	2.264(5)	0.083(12)	0.000
	2.190; 2.034	0.101; 0.289	0.000; 0.000
$O^{13}CS$	1.2609(12)	0.6378(24)	0.065*i*(24)
	−1.274(4)	0.642(2)	0.000
	−1.217; −1.562	0.644; 0.603	0.000; 0.000
$OC^{34}S$	2.1335(7)	0.6655(23)	0.060*i*(25)
	−2.150(4)	−0.655(5)	0.000
	−2.126; −2.603	−0.632; −0.566	0.000; 0.000

[a] The listed uncertainties in the Kraitchman coordinates reflect the sum of both propagated uncertainties from the rotational constants and the Costain error. [b] Each principal axis coordinate has been derived from three sources: the Kraitchman single substitution coordinate ("R_s") is given on the first line, followed by the inertial fit value ("R_0"), and the third line lists the two ab initio values ("R_e", for structures I and II, respectively). The inertial fit value uncertainty encompasses the full range of coordinates obtained from fitting the different sets of moments (see Table 3). [c] Note that only the coordinate's magnitude, and not the sign, is determined from Kraitchman's equations.

An approximate binding energy (E_B) for the complex can be derived from the stretching force constant, k_s, that may itself be calculated by using the pseudodiatomic approximation[23]

$$k_s = \frac{16\pi^4(\mu R_{cm})^2[4B^4 + 4C^4 - (B-C)^2(B+C)^2]}{hD_J} \quad (1)$$

where μ is the pseudodiatomic reduced mass, R_{cm} is the separation between the centers of mass of the OCS and H_2CF_2 monomers ($R_{cm} = 3.41(2)$ Å), B and C are the dimer rotational constants, h is Planck's constant, and D_J is the Watson *S*-reduction distortion constant (easily calculated from the *A*-reduction fitted constants). The resulting value of $k_s = 2.1(1)$ N m^{-1} can then be used in the expression $E_B = (1/72)k_s R_{cm}^2$ (obtained from a Lennard-Jones potential expansion)[24] to estimate a binding energy (E_B) for this complex of 2.1(1) kJ mol^{-1}. Further interpretation of these binding energies will be left until the Discussion section.

Dipole Moment. The dipole moment of the DFM-OCS complex was determined by least-squares fitting a total of 28 experimentally observed Stark shifts (five *M* lobes, belonging to four different rotational transitions) to the dipole moment components, using the QSTARK program[25,26] (resulting in a standard deviation of 6.8 kHz). Due to the *ab* plane of symmetry only the μ_a and μ_b components were expected to be nonzero, so the μ_c dipole component was held fixed at zero—the resulting dipole components are μ_a= 1.1386(18) D, μ_b= 0.4840(63) D, and $\mu_{total} = 1.2372(41)$ D. Including the μ_c component in the fit yields a value of $\mu_c = 0.10(10)$ D and the μ_a and μ_b components remain unchanged within the derived uncertainties (although μ_b and μ_c are heavily correlated in this fit (with a correlation coefficient of 0.96)). The fitted dipole moment components compare well with the ab initio values given in Table 1 and are close to those predicted for structure I, with the μ_a and μ_b components being overestimated by about 0.04 D (3.6% and 6.9%, respectively) by the MP2 calculation. In contrast, the structure II predictions overestimate μ_a and μ_b by 0.14 and 0.72 D, respectively, showing a clear preference for structure I on the basis of dipole moment data.

Projection of the monomer dipole moments (μ(DFM) = 1.97(2) D[27,28] and μ(OCS) = 0.71519(3) D[15]) into the principal axis frame using the best fit structure derived from the inertial fit gives values of $\mu_a = 1.21(2)$ D and μ_b= 0.54(4) D (where the uncertainties take into consideration the variation of the dipole moment projections depending on the different sets of moments of inertia used to fit the structure). A small difference of ∼0.06−0.07 D is evident between the projected and experimental dipole moment components, with both the μ_a and μ_b components being smaller than those calculated from the projection of the monomer moments, suggesting a fairly small induced dipole effect upon complexation.

IV. Discussion

The assignment of the DFM−OCS spectrum completes the series of fluorinated methane complexes with OCS and, along with the first data point from studies of the analogous CO_2 series

TABLE 5: Comparison of Structural Parameters and Binding Energies for the Complete Series of Fluorinated Methane Complexes HCF_3−OCS, H_2CF_2−OCS, and H_3CF−OCS

complex	$R_{C\cdots C}$/Å	R_{CM}/Å[a]	ϕ/deg[b]	E_B/kJ mol^{-1}	$\mu_{monomer}$/D[c]	ref
HCF_3−OCS	3.642(17)	3.965(26)	60.2(4)	1.6(1)	1.65	1
H_2CF_2−OCS	3.582(4)	3.41(2)	64.3(6)	2.1(1)	1.97	this work
H_3CF-OCS	3.75(3)	3.60(3)	61(2)	3.5(1)	1.85	2

[a] R_{CM} is the center of mass separation. [b] ϕ is the OCS tilt angle (O--C$\cdots$C). [c] Dipole moment of the fluorinated methane monomer, taken from ref 27.

($TFM-CO_2$),[3] makes possible some interesting comparisons of their structures, dynamics, and binding. All of these complexes[1–3] exhibit structures in which a hydrogen atom from the substituted methane subunit interacts with the oxygen atom of the OCS or CO_2. TFM−OCS and DFM−OCS exhibited no sign of internal rotation effects in their spectra while $TFM-CO_2$ transitions were split into *A* and *E* states (allowing calculation of a barrier to rotation of the CF_3 group of 30(1) cm^{-1}).[3] At the other extreme, the FM−OCS spectrum showed indications of a very small barrier to rotation of the methyl top (which was manifested in the observed negative P_{cc} planar moments). These observations correlate approximately with the ab initio predictions of the energy differences between the two lowest energy structures I and II (which can be used as a crude estimate of the magnitude of the barrier to rotation, assuming of course that these two structures can be identified as the minimum and the transition state for this motion). For TFM−OCS, the energy difference between the two lowest energy structures (at the ZPE and BSSE uncorrected level) is rather high at 90 cm^{-1}, and this is consistent with the observation of no, or very small, internal rotation splittings in the spectrum. In contrast, predictions for the FM−OCS complex indicated an extremely small energy difference of 0.5 cm^{-1} and this would suggest the possibility of large-amplitude, low-barrier motions in the complex (exactly as was evident experimentally). For DFM−OCS and $TFM-CO_2$ the argument is less clear-cut with these two species having quite similar midrange energy differences between their two lowest energy structures (73 and 75 cm^{-1}, respectively). Internal rotation splittings, consistent with an experimental barrier of 30(1) cm^{-1}, were observed for the $TFM-CO_2$ complex, but no such splittings were evident in the rotational spectrum of DFM−OCS; however, it should be pointed out that internal rotation of the DFM subunit would involve a rotation about an internal C_2 axis rather than a C_3 axis so the DFM−OCS case is fundamentally different from the other members of the series. Clearly, a more rigorous theoretical study of the energetics and dynamics of these complexes (accounting for basis set superposition effects (BSSE) and zero point energy (ZPE) effects) is warranted to see if a quantitatively useful predictive model can be identified; both BSSE and ZPE are expected to have significant effects on the energetics of weak complexes such as those described here. This investigation is planned for a future study, although the current, relatively computationally inexpensive level of calculation does seem to provide a crude estimate of the magnitude of possible internal rotation splittings that might be expected in the experimental measurements.

Inspection of the derived structural properties in an attempt to identify any trends in this series revealed that there is near-perfect correlation between the experimental center of mass separation (R_{CM}) and the dipole moment of the fluorinated methane subunit in the OCS series. The R_{CM} distance decreases as the dipole moment of the methane increases (listed in Table 5, and plotted in Figure 2). Similar correlations for the C$\cdots$C distances, or any sort of correlation between the estimated

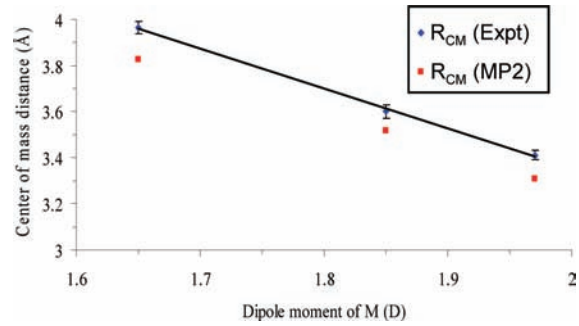

Figure 2. R_{CM} distance versus dipole moment of fluorinated methane (M) in the series of complexes M−OCS. Error bars reflect the experimental uncertainty in the derived R_{CM} distance. The squares indicate the MP2 predicted R_{CM} distances for these complexes.

TABLE 6: Comparison of theoretical (MP2/6-311++G(2d,2p)) and experimental intermolecular distances for the DFM-OCS complex with related complexes.

	$R_{C\cdots C}$/Å		$R_{O\cdots H}$/Å	
complex	MP2	exptl	MP2	exptl
TFM-OCS	3.48	3.642(17)	2.63	2.90(5)
DFM-OCS	3.45	3.58(2)	2.65	2.88(3)
FM-OCS	3.75	3.75(3)	2.65	2.65(6)
$TFM-CO_2$	3.45	3.57(5)	2.70	2.83(5)

binding energy and these parameters is not apparent. Future computational studies will aim to investigate these trends further.

A comparison of predicted structures at the MP2/6-311++G(2d,2p) level across the series (Table 6) shows that although the center of mass separation is consistently underestimated by the MP2 calculation, the linear correlation between this distance and the fluorinated methane dipole moment is still clearly apparent (Figure 2). Note also that although the ab initio calculations do typically tend to underestimate the C$\cdots$C distance, they do reasonably well in predicting the qualitative trends in the C$\cdots$C distances across the series. At the MP2/6-311++G(2d,2p) level they suggest that in the TFM and DFM complexes with OCS (and indeed also for the $TFM-CO_2$ complex), the C$\cdots$C distance is very similar (3.48 and 3.45 Å for the TFM complexes with OCS and CO_2, respectively, and 3.45 Å for the DFM complex), while the distance for the FM−OCS complex is considerably longer (3.75 Å) due to the single F atom lying in the plane rather than having the two F atoms straddling this plane (as they do in the other complexes). This trend in C$\cdots$C distances nicely parallels what is observed experimentally (TFM−OCS,[1] 3.642(17) Å; $TFM-CO_2$,[3] 3.57(5) Å; DFM−OCS, 3.58(2) Å, and FM−OCS, [2] 3.75(3) Å).

For the O$\cdots$H contact distance, the MP2 calculations predict all O$\cdots$H distances to be essentially the same (2.63 Å for TFM−OCS, 2.65 Å for DFM−OCS, 2.65 Å for FM−OCS, and 2.70 Å for $TFM-CO_2$), whereas the experimental numbers show that the O$\cdots$H distances in TFM−OCS, $TFM-CO_2$, and DFM−OCS are somewhat longer than predicted but are nonetheless effectively the same to within the stated uncertainties

TABLE 7: Comparison of Derived Force Constants and Binding Energies for Complexes of Difluoromethane

	k_s/N m^{-1}	E_B/kJ mol^{-1}	ref
Ar	1.45	1.5	10
Xe	1.49	1.8	12
Kr	1.70	1.9	11
OCS	2.1(1)	2.1(1)	this work
DFM dimer	6.25	6.6	6
H_2O	7.7	7.5	8
oxirane	8.3	9.6	4

(2.90(5) Å,[1] 2.83(5) Å,[3] and 2.88(3) Å, respectively) while the FM distance is considerably shorter (2.65(6) Å).[2] Inspection of Tables 5 and 6 does reveal that the experimental O···H separation decreases as the binding energy increases, although the differences are small, particularly between the TFM and DFM complexes. It should be noted, however, that given the perturbations in the FM−OCS spectrum arising from the low-barrier motion of the MeF subunit, and the approximations inherent in the calculation of the binding energy for all complexes, the trends identified from this analysis may be somewhat fortuitous.

Table 5 contains comparisons of estimated binding energies, distances, and angles involving OCS. Note that the OCS tilt angle (ϕ) is very similar in all three complexes and the binding energy of the OCS complexes increases along the series in the order TFM < DFM < FM despite the decreasing trend in dipole moments (DFM > FM > TFM). A comparison of force constants (k_s) and binding energies (E_B) for the DFM−OCS complex with other fluorinated methane−OCS complexes, as well as with other DFM complexes, is listed in Table 7. It is clear that the DFM−OCS complex is the weakest bound in the series, more in line with the energies typically associated with the rare gas complexes of DFM.

V. Conclusions

Rotational spectra have been measured and fit to a semirigid Watson *A*-reduction Hamiltonian for four isotopologues of the DFM−OCS weakly bound dimer. From the experimental P_{cc} values, it was determined that the two fluorine atoms, and not the two hydrogen atoms, lie out of that plane leading us to favor structure I (Figure 1) as the experimentally observed structure for this complex. Comparison of the structural parameters of this and other fluorinated methane complexes with OCS have revealed similarities in the intermolecular distances within the series, and a correlation between the dipole moment of the fluorinated methane monomer and the R_{CM} distance has been identified.

The effects of the changing polarity of the C−H bonds of the substituted methane on the structural parameters of the complex are not clearly discernible in this series. The C−H bond polarity would be expected to decrease with decreasing fluorination, in the order TFM > DFM > FM, although because of the relative alignment of the C−H and C−F bonds within the monomers, the overall monomer dipole moments actually follow the trend DFM > FM > TFM. However, a decrease in the R_{CM} distance as the dipole moment of the fluorinated methane increases indicates that dipole−dipole interactions do appear to dominate the structures of this series of complexes. It is interesting to note that a trend between the derived experimental O···H distance and the derived binding energy can also be seen (with the O···H distance decreasing as the binding energy increases).

Due to the relative alignment of the two monomers in the members of this series there are some structural differences: the DFM and TFM monomers are able to complex with OCS aligning such that the F atoms straddle the symmetry plane, while in the FM complex, the F atom is necessarily located in the symmetry plane, leading to an increased C···C distance relative to the other members of the series; this makes direct comparison between the structural parameters somewhat more problematic.

It is hoped that this series of experimental measurements can serve as benchmarks for computational calculations to promote a better understanding of the optimum level of theory for modeling such weak complexes and obtaining accurate predictions of their dynamic properties. A more comprehensive computational study on this series of complexes both to probe the nature of any interaction between the O and H atoms of the two subunits (using natural bond orbital (NBO) analysis,[29] for example), as well as to investigate of the effects of BSSE and ZPE corrections, the level of theory and basis sets, and to perform anharmonic frequency calculations to provide theoretical centrifugal distortion constants, is currently underway.

Acknowledgment. The authors acknowledge the donors of the ACS Petroleum Research Fund (PRF no. 39752-GB6) for support of this work. The authors also thank Dr. Rebecca Peebles for useful suggestions during the preparation of the manuscript.

Supporting Information Available: Tables of measured transition frequencies for the normal and three additional isotopic species. This material is available free of charge via the Internet at http://pubs.acs.org.

References and Notes

(1) Serafin, M. M.; Peebles, S. A. *J. Phys. Chem. A* **2006**, *110*, 11938.
(2) Serafin, M. M.; Peebles, S. A. *J. Phys. Chem. A* **2008**, *112*, 1473.
(3) Serafin, M. M.; Peebles, R. A.; Peebles, S. A. *J. Mol. Spectrosc.* **2008**, *250*, 1.
(4) Blanco, S.; López, J. C.; Lesarri, A.; Caminati, W.; Alonso, J. L. *ChemPhysChem* **2004**, *5*, 1779.
(5) Blanco, S.; López, J. C.; Lesarri, A.; Alonso, J. L. *J. Mol. Struct.* **2002**, *612*, 255.
(6) Caminati, W.; Melandri, S.; Moreschini, P.; Favero, P. G. *Angew. Chem., Intl. Ed. Engl.* **1999**, *38*, 2924.
(7) Caminati, W.; Melandri, S.; Schnell, M.; Banser, D.; Grabow, J.-U.; Alonso, J. L. *J. Mol. Struct.* **2005**, *742*, 87.
(8) Caminati, W.; Melandri, S.; Rossi, I.; Favero, P. G. *J. Am. Chem. Soc.* **1999**, *121*, 10098.
(9) Blanco, S.; Melandri, S.; Ottaviani, P.; Caminati, W. *J. Am. Chem. Soc.* **2007**, *129*, 2700.
(10) López, J. C.; Favero, P. G.; Dell′Erba, A.; Caminati, W. *Chem. Phys. Lett.* **2000**, *316*, 81.
(11) Maris, A.; Melandri, S.; Caminati, W.; Rossi, I. *Chem. Phys. Lett.* **2005**, *407*, 192.
(12) Caminati, W. *J. Phys. Chem. A* **2006**, *110*, 4359.
(13) Balle, T. J.; Flygare, W. H. *Rev. Sci. Instrum.* **1981**, *52*, 33.
(14) Grabow, J.-U. Ph.D. Thesis, University of Kiel, 1992.
(15) Reinartz, J. M. L. J.; Dymanus, A. *Chem. Phys. Lett.* **1974**, *24*, 346.
(16) Frisch, M. J.; Trucks, G. W.; Schlegel, H. B.; Scuseria, G. E.; Robb, M. A.; Cheeseman, J. R.; Montgomery J. A., Jr.; Vreven, T.; Kudin, K. N.; Burant, J. C.; Millam, J. M.; Iyengar, S. S.; Tomasi, J.; Barone, V.; Mennucci, B.; Cossi, M.; Scalmani, G.; Rega, N.; Petersson, G. A.; Nakatsuji, H.; Hada, M.; Ehara, M.; Toyota, K.; Fukuda, R.; Hasegawa, J.; Ishida, M.; Nakajima, T.; Honda, Y.; Kitao, O.; Nakai, H.; Klene, M.; Li, X.; Knox, J. E.; Hratchian, H. P.; Cross, J. B.; Bakken, V.; Adamo, C.; Jaramillo, J.; Gomperts, R.; Stratmann, R. E.; Yazyev, O.; Austin, A. J.; Cammi, R.; Pomelli, C.; Ochterski, J. W.; Ayala, P. Y.; Morokuma, K.; Voth, G. A.; Salvador, P.; Dannenberg, J. J.; Zakrzewski, V. G.; Dapprich, S.; Daniels, A. D.; Strain, M. C.; Farkas, O.; Malick, D. K.; Rabuck, A. D.; Raghavachari, K.; Foresman, J. B.; Ortiz, J. V.; Cui, Q.; Baboul, A. G.; Clifford, S.; Cioslowski, J.; Stefanov, B. B.; Liu, G.; Liashenko, A.; Piskorz, P.; Komaromi, I.; Martin, R. L.; Fox, D. J.; Keith, T.; Al.Laham, M. A.; Peng, C. Y.; Nanayakkara, A.; Challacombe, M.; Gill, P. M. W.; Johnson, B.; Chen, W.; Wong, M. W.; Gonzalez, C.; Pople, J. A. *Gaussian 03*; Gaussian, Inc.: Wallingford, CT, 2004.

(17) Pickett, H. M. *J. Mol. Spectrosc.* **1991**, *148*, 371.
(18) Hirota, E. *J. Mol. Spectrosc.* **1978**, *71*, 145.
(19) Harmony, M. D.; Laurie, V. W.; Kuczkowski, R. L.; Schwendeman, R. H.; Ramsay, D. A.; Lovas, F. J.; Lafferty, W. J.; Maki, A. J. *J. Phys. Chem. Ref. Data* **1979**, 8.
(20) Schwendeman, R. H. In *Critical Evaluation of Chemical and Physical Structural Information*; Lide, D. R., Paul, M. A., Eds.; National Academy of Sciences: Washington, DC, 1974. The STRFITQ program used in this work is the University of Michigan modified version of Schwendeman′s original code.
(21) Kraitchman, J. *Am. J. Phys* **1953**, *21*, 17.
(22) Kraitchman coordinates and propagated errors were calculated using the KRA code, Kisiel, Z. "PROSPE—Programs for Rotational Spectroscopy" available at http://info.ifpan.edu.pl/kisiel/prospe.htm.
(23) Millen, D. *J. Can. J. Chem* **1985**, *63*, 1477.
(24) Read, W. G.; Campbell, E. J.; Henderson, G. *J. Chem. Phys.* **1983**, *78*, 3501.
(25) Kisiel, Z.; Kosarzewski, J.; Pietrewicz, B. A.; Pszczółkowski, L. *Chem. Phys. Lett.* **2000**, *325*, 523.
(26) Kisiel, Z."PROSPE—Programs for Rotational Spectroscopy" available at http://info.ifpan.edu.pl/kisiel/prospe.htm, accessed June 2008.
(27) Nelson, R. D.; Lide, D. R.; Maryott, A. A. NSRDS 10 Selected Values of Electric Dipole Moments for Molecules in the Gas Phase. NSRDS-NBS **1967**, *10*.
(28) Lide, D. R. *J. Am. Chem. Soc.* **1952**, *74*, 3548.
(29) Weinhold, F.; Landis, C. R. *Valency and Bonding: A Natural Bond Orbital Donor-Acceptor Perspective*; Cambridge University Press: Cambridge, UK, 2005.

JP8072393